Contrib Mineral Petrol (1993) 114:148–159

Contributions to Mineralogy and Petrology

Exsolution of garnet within clinopyroxene of mantle eclogites: major- and trace-element chemistry

Eric A. Jerde[1], Lawrence A. Taylor[1], Ghislaine Crozaz[2], and Nikolai V. Sobolev[3]

[1] Department of Geological Sciences, University of Tennessee, Knoxville, TN 37996, USA
[2] Earth and Planetary Sciences Department and McDonnell Center for the Space Sciences, Washington University, St. Louis, MO 63130, USA
[3] Institute of Mineralogy and Petrography, Siberian Branch of the Russian Academy of Sciences, Novosibirsk, Russia

Received August 3, 1992 / Accepted November 12, 1992.

Abstract. Eclogite xenoliths from the mantle have experienced a wide variety of processes and *P-T* conditions, many of which are recorded in the mineral compositions and textures. Exsolution of garnet from clinopyroxene is one such texture, occurring in a minority of mantle eclogites. New analyses of clinopyroxene and garnet of eclogite xenoliths from kimberlites at Bellsbank (South Africa) and Obnazhënnaya (Yakutia, Russia) are presented here, and these are combined with data from the literature. Exsolution of garnet from clinopyroxene is generally lamellar, although lens-shaped garnets are also present. Major- and trace-element characteristics show a wide range of compositions and include eclogite Groups A, B, and C. Rare-earth element (REE) concentrations of garnet and pyroxene were determined by SIMS, and the REE patterns are subtly different from those in "ordinary" eclogites. Differences include the absence of prominent Eu anomalies in samples of this study and differences in the slopes of chondrite-normalized REE patterns. It is possible that these "signatures" are unique to exsolved eclogites, a result of subsolidus elemental partitioning during exsolution. Some reconstructed whole-rock compositions are aluminuous; comparison with ordinary eclogites shows only minor differences, implying a similar origin. If the immediate precursor to the exsolved eclogites was a monomineralic pyroxenite, the excess aluminium was tied up in Tschermak's molecule, although the occasional presence of kyanite exsolution lamellae is indicative of a Ca-Eskola component. Reconstructed "pyroxenes" from kyanite- and corundum-rich samples contain unrealistic amounts of aluminium for mantle pyroxenes. A protolith (or parental pyroxene) "threshold" of $\sim 24\%$ Al_2O_3 may exist, above which (as in a plagioclase cumulate) the final assemblage is kyanite- and/or corundum-bearing.

Introduction

Eclogite xenoliths in kimberlites and alkali basalts are of great interest for they have been transported from the mantle, providing a means of direct sampling of this relatively unknown portion of the earth. Among the population of eclogite xenoliths, some are observed to contain garnet exsolution from clinopyroxene (e.g., Sobolev and Sobolev 1964; Harte and Gurney 1975; Lappin and Dawson 1975; Lappin 1978; Smyth et al. 1984, 1989). Garnet exsolution was documented to be predominantly parallel to {100} of clinopyroxene by Aoki et al. (1980) in a pyroxenite nodule. Using single-crystal X-ray diffraction, they confirmed an origin of the lamellar garnet by exsolution directly from clinopyroxene as opposed to recrystallization from other precursor phases. A variety of orientations may be present, however, as described by Desnoyers (1975). The first discussion of an origin for this exsolution was by Sobolev and Sobolev (1964), who suggested that this texture was formed by an increase in pressure. Green (1966) demonstrated that many Hawaiian eclogites contain aluminous clinopyroxenes which crystallized from an alkaline magma at mantle pressure and subsequently exsolved garnet (plus orthopyroxene). Harte and Gurney (1975) assumed a high-pressure igneous origin and considered the extensive garnet exsolution from clinopyroxene to indicate a large temperature decrease and possible pressure increase. For a kyanite-bearing eclogite, Lappin and Dawson (1975) also proposed an origin by cooling during a tectonically controlled pressure increase.

Through the use of Nd and Sr isotopes, Jagoutz (1988) concluded that garnet exsolution from clinopyroxene in an eclogite xenolith from the Vissury kimberlite (Tanzania) took place in an essentially closed system and was controlled by diffusional processes during cooling. For some kyanite-eclogite and grospydite (grossular(gros)-pyroxene(py)-disthene(di) [kyanite] eclogite (Bobrievich et al. 1960; grossular $> 50\%$) xenoliths from the Bellsbank kimberlite, Smyth et al. (1984, 1989) concluded that the exsolution occurred on cooling from near-solidus temperatures at pressures in excess of 30 kbar. Sobolev and Sobolev (1964) proposed initial exsolution of orthopyroxene from clinopyroxene followed by recrystallization of the orthopyroxene (+ spinel, clinopyroxene, quartz) to garnet; a similar conclusion reached by Borley and Sud-

Correspondence to: E.A. Jerde

daby (1975) for some pyroxenite nodules from the Jagersfontein kimberlite. Processes capable of producing garnet exsolution textures through removal of the Tschermak component (CaTs) of pyroxene are varied. The solubility of CaTs in pyroxene decreases with increasing pressure and decreasing temperature (e.g. Hays 1966; Gasparik 1984). Therefore, any process involving a pressure increase or temperature decrease (or a combination of the two) may result in garnet exsolution from pyroxene.

The principal aim of this paper is an initial examination of the rare-earth elements (REE) in eclogites exhibiting garnet exsolution from clinopyroxene. These data will be integrated with those from previous eclogite studies, with the goal of shedding light on differences (if any) between trace elements in eclogites with exsolution and in those with no lamellae. Previously, REE data for only two eclogites with garnet exsolution textures have been presented (Caporuscio and Smyth 1990). A search through our collection of eclogite xenoliths yielded several with garnet exsolution textures. Major-element results are presented herein for five eclogites with exsolution textures from Bellsbank, South Africa and three from Obnazhënnaya, Siberia; REE compositions are given for four of the Bellsbank xenoliths. The REE were obtained by SIMS for unaltered portions of mineral grains. For the purposes of discussion, eclogites with garnet exsolution textures will be referred to as "exsolved" eclogites, those without such textures as "ordinary" eclogites.

Petrography

Garnet (1–5 mm) and clinopyroxene (1–15 mm) form coarser portions of the eclogite samples and, though recrystallized and reequilibrated by subsolidus metamorphic processes, may represent the original minerals in some samples. Three of the eight samples presented here are bimineralic, garnet-clinopyroxene eclogites (with the exception of orthopyroxene lamellae in clinopyroxene in one sample and the occurrence of accessory phases). The three samples from Obnazhënnaya (splits of sample) O-160 described in Sobolev 1977) and two from Bellsbank (PHN34203 and PHN2793-3a) contain abundant corundum. In another Bellsbank sample (PHN34215), accessory rutile occurs as inclusions in garnet and clinopyroxene. Typically, garnet occurs both as lamellae or as discontinuous blebs exsolved from clinopyroxene and as coarser crystals, both internal and external to clinopyroxene. Lamella and blebs are typically parallel to each other and probably have the same origin, with a continuum existing between the two morphologies. The garnet between clinopyroxene grains is generally crescent to lens shaped. Locally, lamellar garnet appears to merge into larger, xenomorphic inclusions. Textural relationships indicate that the lamellar garnet exsolved from clinopyroxene, as did the lamellae of orthopyroxene. Such relationships include consistent crystallographic orientation of lamellae in clinopyroxene and the parallelism of most garnet lamellae to orthopyroxene lamellae. Secondary phases are present, including serpentine, phlogopite, ilmenite, and amphibole, formed as alteration products of the high *P-T* assemblage. Kyanite exsolution from clinopyroxene, seen here mainly in the O-160 samples, is not unusual in eclogites (e.g., Carswell et al. 1981; Smyth et al. 1984, 1989). As with garnet, it is found as blebs, lenses, and discrete grains within eclogites, and it has been shown to be epitaxial with the host clinopyroxene (Smyth et al. 1984) with coherent grain boundaries (McCormick 1984).

Detailed point counts of all phases, including products of secondary alteration, were made. Using textural criteria, a specific primary mineral was assigned to each occurrence of a secondary phase. In this way, the observed modes were used to construct "original" (post-exsolution, pre-alteration) modal mineralogies (Table 1). The degree of alteration present in the samples is significant (Table 1), but in all cases is less than 50% and does not preclude the determination of original textures and mineral assemblages. In addition, the REE analyses made by SIMS on unaltered cores provide compositions essentially unaffected by alteration, allowing conclusions to be drawn concerning pre-metasomatic mantle chemistry. Detailed sample descriptions are given in the appendix.

Major elements and classification

Three groups (A, B, and C) of eclogites originally were proposed based on mode of occurrence (Coleman et al. 1965), one of these (Group A) was postulated to have a mantle origin. Using major- and trace-element compositions, as well as isotopic systematics, these groups were put into a chemical framework and applied to mantle xenoliths by later workers (i.e., Shervais et al. 1988; Taylor and Neal 1989; Neal et al. 1990), who suggested an oceanic crustal origin for Groups B and C from Bellsbank, South Africa. With respect to the mineralogy, Group A eclogites contain garnets and clinopyroxenes rich in Mg and Cr, with the clinopyroxenes possessing a low jadeite component (exemplified by Na). Group B eclogites typically contain garnet rich in Fe and clinopyroxenes of intermediate jadeite. Group C eclogites have Ca-rich garnets and clinopyroxenes rich in the jadeite component. This scheme can be used to classify most eclogites based on mineral chemistry alone (Shervais et al. 1988; Taylor and Neal 1989) and provides an effective means to distinguish and classify samples for further isotopic and chemical study.

Examples of *eclogite containing garnet exsolution from clinopyroxene are found from all three groups.* The process that caused this exsolution bears directly on the pressure-temperature paths and tectonic histories of the various samples. The presence of similar features in samples with contrasting (i.e., crustal vs mantle) protoliths implies similar subsolidus processes and *P-T* histories common to eclogites derived from diverse progenitors. As a result, the presence or absence of exsolution may place few or no constraints on the earlier igneous petrogenesis of a given sample.

Major-element compositions were determined by electron microprobe analysis using the four-spectrometer CAMECA SX-50 in the Department of Geological Sciences at the University of Tennessee. The accelerating voltage was 15 kV, with beam currents of 20 or 30 nA. The beam size was 5 or 10 microns, and counting times of 20 seconds were used for all elements and backgrounds, except for Na in garnet and K in clinopyroxene (40 seconds). All data were corrected using ZAF procedures. Average compositions for garnet and clinopyroxene are listed in Tables 2 and 3. Both garnets and clinopyroxene in the "PHN" samples from South Africa are homogeneous with no appreciable zoning. This homogeneity is present throughout each section and among all crystals from exsolved lamellae to primary grains. This is in contrast to inhomogeneities reported in intergrowths within Roberts Victor grospydites (Harte and Gurney 1975; Sautter and Harte 1988).

Table 1. Estimates of observed and reconstructed primary modal compositions

Observed

Sample	Garnet	Clinopyroxene	Orthopyroxene	Corundum	Kyanite	Clinopyroxene2	Phlogopite (garnet)	Phlogopite (clinopyroxene)	Serpentine (clinopyroxene)	Other[a]
PHN2791-a	42.3	36.1	–	–	–	3.6	13.2	4.8	–	tr.
PHN34195	12.6	66.8	6.1	–	–	–	2.3	10.9	1.3	tr.
PHN34215	20.4	41.4	–	–	–	3.1	9.4	23.7	0.6	1.4
PHN34203	41.9	36.5	–	3.2	–	–	5.0	13.4	–	–
PHN2793-3a	25.7	37.7	–	5.5	tr.	–	9.3	16.9	4.9	–
O-160a	7.6	44.0	–	19.5	3.2	–	9.6	16.1	–	–
O-160b	12.6	43.3	–	20.3	5.3	–	5.3	9.4	3.8	–
O-160c	13.1	48.6	–	10.7	4.7	–	7.2	10.7	5.0	–

Reconstructed primary exsolved assemblage

Sample	Garnet	Clinopyroxene	Corundum	Kyanite
PHN2791-a	55.5	44.5	–	–
PHN34195	14.9	85.1	–	–
PHN34215	29.8	70.2	–	–
PHN34203	46.9	49.9	3.2	–
PHN2793-3a	35.0	59.5	5.5	tr.
O-160a	17.2	60.1	19.5	3.2
O-160b	17.9	56.5	20.3	5.3
O-160c	20.3	64.3	10.7	4.7

tr., trace

[a] Includes opaque minerals (ilmenite) in the alteration assemblage of clinopyroxene, green amphibole as an alteration of clinopyroxene (PHN34215, 0.8%), and accessory rutile (PHN34215, 0.1%)

The Obnazhënnaya samples (O-160a, b, c) show inhomogeneities as well, as shown in Tables 2 and 3. In general, single grains are homogeneous, with variation observed between the grains in a single sample. There are cases, however, where pyroxene shows a compositional gradient adjacent to a garnet lamella, with Al_2O_3 varying by up to 1% absolute. These rare gradients are preserved diffusion gradients akin to those described by Sautter and Harte (1988), although localized, being present over 100 μm or less, and not as severe. Other elements (e.g., Cr, Ti, Fe) do not display significant gradients in the clinopyroxene. This is likely due to the slower diffusion of Al through the pyroxene relative to other cations. The preservation of such diffusion gradients can reflect either a rapid cooling rate in the mantle to temperatures below those that effectively halt diffusion or a short residence time following garnet exsolution (Sautter and Harte 1988) and sampling as a xenolith a relatively short time after exsolution took place. The relative garnet homogeneity and the pyroxene inhomogeneity are consistent with experimental evidence indicating a faster equilibration rate for garnet than pyroxene (e.g., Freer et al. 1982; Sautter and Harte 1988, 1990). The inhomogeneity in composition of the various garnet grains is less pronounced in O-160b, suggesting that partial reequilibration has occurred in this portion of the xenolith. The differences between the various portions of a single xenolith (O-160b was obtained ~3 cm from O-160a) are likely due to kinetic effects rather than varying conditions across the xenolith itself. Such effects are reflected in the fact that Al is the only element exhibiting gradients; presumably the other cations had sufficient time to equilibrate.

Garnets in samples PHN2791-a, PHN34195, and PHN34215 are rich in Mg; those in PHN34203, PHN2793-3a, and the O-160 samples are Ca-rich. The compositions are shown in Fig. 1 along with data from Taylor and Neal (1989) for comparison. Samples O-160 contain garnet with grossular components > 50 mol%, abundant corundum, and kyanite, and are classified as corundum grospydite.

Clinopyroxene compositions are shown in Fig. 2, along with the group boundaries of Taylor and Neal (1989). The eight samples of this study fall into all three of the eclogite groups: PHN34203 and 2793-3a in Group C, the three O-160 samples in Group B, and the other three are Group A. It is notable that the Ca-rich garnets of O-160 (Table 2; grossular > 50 mol %) exhibit compositions more typical of group C to which most grospydites belong. This discrepancy may be an indication that the classification scheme of Taylor and Neal (1989) is insufficient. The pyroxene scheme of Taylor and Neal (1989) is directed at the eclogites of southern Africa, and the application to eclogites of the Siberian platform may be inappropriate, evidence that the Siberian eclogites may be fundamentally different from their African counterparts. Another possibility is that disequilibrium is confusing the classification of O-160. It has been suggested that after garnet exsolution, the Ca in garnet reequilibrates while

Table 2. Mean composition of analyzed garnet

Sample	PHN2791-a	PHN34195	PHN34215	PHN34203	PHN2793-3a
SiO_2[a]	40.6 (2)[b]	41.0 (3)	41.3 (1)	39.9 (1)	39.7 (2)
TiO_2	0.06 (2)	0.10 (1)	0.09 (1)	0.12 (1)	0.13 (1)
Al_2O_3	23.2 (2)	23.1 (2)	23.1 (1)	22.6 (1)	22.6 (1)
Cr_2O_3	0.10 (4)	0.54 (8)	0.46 (8)	0.04 (2)	0.03 (2)
FeO_t	12.4 (2)	12.4 (2)	12.3 (2)	8.62 (15)	9.45 (14)
MnO	0.42 (5)	0.41 (1)	0.40 (1)	0.19 (3)	0.19 (3)
MgO	16.5 (5)	18.5 (2)	18.3 (1)	6.91 (5)	7.80 (8)
CaO	6.58 (71)	4.18 (6)	4.16 (4)	21.2 (1)	19.8 (2)
Na_2O	0.04 (3)	0.03 (8)	0.03 (1)	0.04 (2)	0.04 (1)
Total	99.90	100.26	100.14	99.62	99.74

Sample	O-160a_1	O-160a_2	O-160-b_1	O-160b_2	O-160c_1	O-160c_2
SiO_2	39.8 (4)	40.8 (2)	40.4 (5)	40.0 (3)	40.0 (2)	41.2 (5)
TiO_2	< 0.03	< 0.03	0.03 (1)	< 0.03	< 0.03	< 0.03
Al_2O_3	23.0 (2)	23.0 (1)	23.1 (1)	23.0 (1)	23.0 (1)	23.6 (1)
Cr_2O_3	0.04 (2)	0.03 (2)	0.06 (3)	0.05 (4)	< 0.03	0.04 (1)
FeO_t	4.61 (7)	6.30 (8)	4.67 (12)	5.09 (7)	4.66 (8)	5.78 (7)
MnO	0.08 (2)	0.14 (4)	0.10 (3)	0.08 (4)	0.09 (1)	0.09 (1)
MgO	8.07 (10)	11.0 (3)	8.26 (18)	8.79 (11)	8.03 (6)	13.4 (9)
CaO	23.7 (1)	18.9 (3)	23.5 (3)	22.7 (3)	23.8 (1)	16.0 (10)
Na_2O	< 0.03	< 0.03	< 0.03	< 0.03	< 0.03	< 0.03
Total	99.30	100.17	100.02	99.71	99.58	100.11

[a] Oxide concentration are in percent (average of at least five analyses)
[b] Units in ( ) represent one standard deviation of replicate analyses in terms of least units cited

Table 3. Mean compositions of analyzed pyroxene

Sample	PHN2791-a	PHN34195	PHN34195[c]	PHN34215	PHN34203	PHN2793-3a
SiO_2[a]	54.5 (2)[b]	54.6 (1)	57.3 (2)	54.7 (1)	55.1 (3)	55.1 (4)
TiO_2	0.12 (2)	0.15 (1)	0.05 (2)	0.15 (2)	0.09 (2)	0.12 (2)
Al_2O_3	3.63 (18)	2.84 (3)	0.44 (3)	2.87 (4)	18.0 (2)	18.1 (4)
Cr_2O_3	0.12 (3)	0.44 (5)	< 0.03	0.38 (5)	< 0.03	0.03 (3)
FeO_t	2.49 (8)	2.72 (7)	7.57 (7)	2.65 (6)	1.08 (5)	1.19 (7)
MnO	0.04 (3)	0.07 (3)	0.13 (1)	0.04 (2)	< 0.03	< 0.03
MgO	15.2 (2)	15.7 (1)	34.2 (2)	15.5 (1)	6.01 (6)	5.97 (22)
CaO	21.2 (2)	21.1 (1)	0.29 (2)	21.0 (1)	10.7 (1)	10.6 (3)
Na_2O	2.12 (8)	1.94 (3)	0.04 (1)	1.90 (4)	8.38 (9)	8.29 (42)
K_2O	< 0.03	< 0.03	< 0.03	< 0.03	< 0.03	< 0.03
Total	99.42	99.56	100.02	99.19	99.36	99.40

Sample	O-160a_1	O-160a_2	O-160-b_1	O-160b_2	O-160c_1	O-160c_2
SiO_2	49.5 (2)	52.1 (3)	48.6 (3)	52.4 (3)	50.9 (4)	52.1 (2)
TiO_2	0.04 (1)	0.04 (2)	0.04 (1)	0.04 (1)	0.05 (2)	0.03 (1)
Al_2O_3	16.2 (2)	13.3 (1)	17.8 (1)	13.4 (2)	14.9 (1)	13.1 (3)
Cr_2O_3	0.03 (2)	0.04 (1)	0.07 (1)	0.05 (2)	0.05 (2)	0.03 (2)
FeO_t	0.97 (10)	0.95 (7)	0.93 (1)	0.86 (2)	0.94 (6)	0.96 (7)
MnO	< 0.03	< 0.03	< 0.03	< 0.03	< 0.03	< 0.03
MgO	9.78 (10)	10.5 (1)	9.02 (7)	10.4 (2)	9.99 (8)	10.6 (2)
CaO	19.4 (3)	18.0 (2)	18.8 (1)	17.6 (2)	17.8 (7)	18.0 (2)
Na_2O	3.60 (7)	4.46 (12)	3.90 (2)	4.56 (7)	4.00 (31)	4.32 (13)
K_2O	< 0.03	< 0.03	< 0.03	< 0.03	< 0.03	< 0.03
Total	99.52	99.39	99.16	99.31	98.63	99.14

[a] Oxide concentrations are in percent (average of at least five analyses)
[b] Units in ( ) represent one standard deviation of replicate analyses in terms of least units cited
[c] Orthopyroxene in lamellae exsolved from clinopyroxene

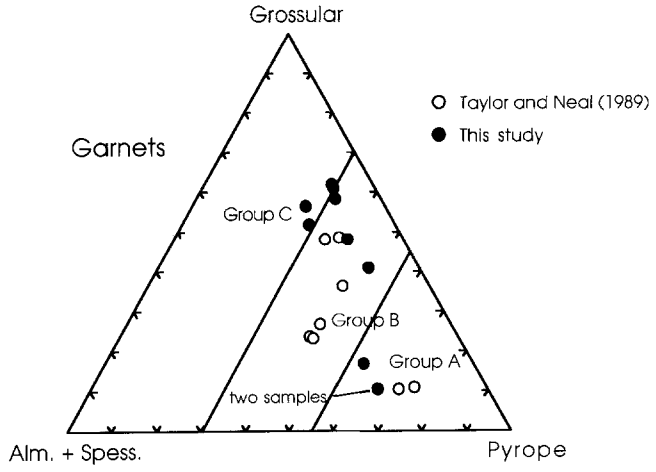

Fig. 1. Ca-Mg-Fe diagram for garnets of this study and those of Taylor and Neal (1989) showing the separation of eclogites into three groups. The boundary lines for the classification of Coleman et al. (1965) are shown for reference

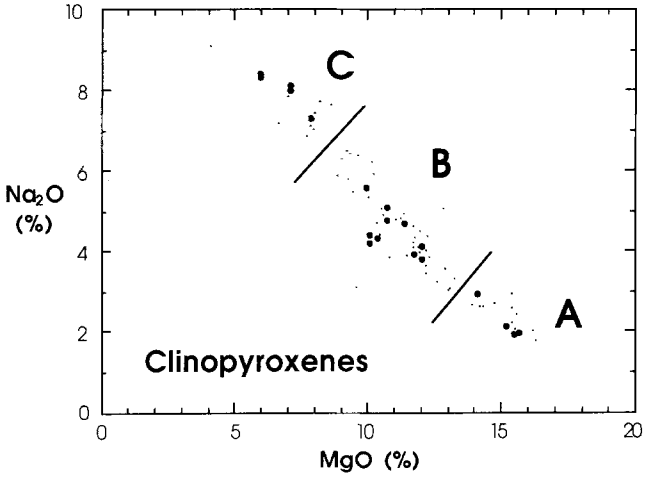

Fig. 2. Na_2O versus MgO diagram for clinopyroxene showing the separation of eclogite groups (after Taylor and Neal 1989). Highlighted samples are those of this study as well as the eleven samples from Smyth and Caporuscio (1984) containing garnet exsolution

that in the clinopyroxenes does not (Sautter and Harte 1988), and this is "frozen-in" by lowering of the temperature. Similar ambiguities between garnet and clinopyroxene are present among other eclogites from Yakutia currently being studied. This demonstrates that this classification scheme should be used as an initial discriminator only. Many other factors (i.e., trace elements, isotopes) must be considered in a final assessment of eclogite type.

Trace elements

Trace-element (REE) analyses of garnet and clinopyroxene were made on thin sections with a modified CAMECA IMS-3f ion microprobe at Washington University. Details of the analytical procedures are given in Zinner and Crozaz (1986) and Lundberg et al. (1988, 1990). The reference element for clinopyroxene and garnet in this study was Si. The relative abundances of twenty other elements were monitored. Within each sample, the minerals were homogeneous across the section, and no REE compositional differences were found between garnet observed as equant grains or exsolved lamellae. The REE compositions are given in Table 4, and the rare-earth patterns for the samples analyzed here along with those of two exsolved samples of Smyth and Caporuscio (1984) for which there are REE data (Caporuscio and Smyth 1990) are shown in Fig. 3A, B. Only two of the Group A samples were analyzed (PHN 2791-a was not). It must be noted that the data of Caporuscio and Smyth (1990) for SBB-2H and SBB-3H (Fig. 3) are INAA data and comparison with SIMS data may be misleading. Because INAA relies on mineral separations, tiny amounts of contamination may affect results, while the SIMS procedure should eliminate effects of metasomatism from the resulting compositions. Metasomatism can have a multitude of imprints, and attempts to subtract these imprints often have ambiguous results. In addition, there is evidence that washing and acid leaching can remove REE and may change the La/Yb ratio in some minerals (Jagoutz et al. 1980; Kurat et al. 1980; Stosch 1982). The great strength of SIMS analysis is that it provides a means of looking past these potential effects, allowing a direct discussion of mantle chemistry. However, only six eclogites with exsolution have been analyzed for REE, and the two analyzed by INAA are included in the discussions for completeness. In fact, the only mineral REE analysis of a Group B eclogite with exsolution is among the INAA data of Caporuscio and Smyth (1990).

The REE contents of the samples correspond to the eclogite groups indicated by Taylor and Neal (1989), who found Group A clinopyroxenes enriched in LREE relative to Group C ($> 100 \times$ chondrites for Group A vs roughly chondritic for Group C) and Group C garnets enriched in HREE relative to Group A ($100 \times$ chondrites vs $10 \times$ chondrites). Note that two eclogites, PHN34195 and PHN34215, have essentially identical REE patterns. In two other samples analyzed here (PHN34203 and PHN2793-3a), clinopyroxene LREE have an abrupt change in slope at Sm, which is possibly due to uncertainties involved in the analysis of samples with such low REE abundances, although this slope change is not seen in other clinopyroxenes with similarly low REE abundances (Fig. 3D). In addition, a similar slope change also exists in one of the samples (SBB-2H) analyzed by Caporuscio and Smyth (1990). No definite Eu anomaly exists in any of the exsolved eclogites. A positive anomaly may be present in SBB-3H, nominally a Group B eclogite, although the lack of Gd data precludes certainty. Data for ordinary eclogites can show definite positive Eu anomalies, in both Group B and Group C eclogites (Fig. 3C, D).

Also interesting is the steep negatively sloped pattern for the lightest REE, in clinopyroxenes from PHN34195 and PHN34215, with a relatively flat pattern from Nd to Lu. The Sm values are typical of clinopyroxenes for Group A eclogites (e.g., Jagoutz 1988; Taylor and Neal 1989), but the LREE slopes are greater than those shown by Taylor and Neal (1989). In addition, the middle and heavy REE are enriched by as much as a factor of 5, which results in chondrite normalised values of $La_N/Yb_N \sim 75$ in

Table 4. Rare earth concentrations (in ppm) of garnet and clinopyroxene

	PHN34195 (A)		PHN34215 (A)		PHN34203 (C)		PHN2793-3a (C)	
	Garnet	Clinopyroxene	Garnet	Clinopyroxene	Garnet	Clinopyroxene	Garnet	Clinopyroxene
La	0.021(5)	40.9(6)	0.025(3)	41.7(3)	0.093(8)	0.29(2)	0.143(8)	0.37(3)
Ce	0.085(12)	35.3(6)	0.082(10)	35.7(3)	0.58(5)	0.68(4)	0.67(3)	0.58(4)
Pr	0.014(3)	1.30(9)	0.014(2)	1.36(5)	0.14(1)	0.047(7)	0.076(5)	0.033(4)
Nd	0.10(1)	2.7(1)	0.074(6)	2.59(6)	0.64(3)	0.139(9)	0.24(1)	0.050(6)
Sm	0.17(2)	1.0(1)	0.14(1)	1.11(5)	0.10(1)	0.008(8)	0.39(2)	0.028(7)
Eu	0.10(1)	0.34(2)	0.105(8)	0.34(1)	0.080(6)	0.004(1)	0.25(1)	0.009(2)
Gd	1.4(1)	1.9(2)	1.32(8)	1.99(8)	0.65(7)	0.022(6)	1.46(4)	0.021(5)
Tb	0.57(6)	0.31(3)	0.50(4)	0.32(2)	0.22(2)	0.002(1)	0.33(2)	0.005(2)
Dy	6.4(3)	1.88(9)	6.6(2)	2.01(5)	2.32(9)	0.017(3)	3.42(8)	0.021(4)
Ho	1.9(1)	0.28(2)	2.0(1)	0.32(2)	0.67(5)	0.004(1)	0.90(3)	0.002(1)
Er	7.0(3)	0.72(5)	8.1(2)	0.75(3)	2.19(9)	0.010(3)	2.95(6)	0.009(3)
Tm	1.1(1)	0.062(9)	1.48(8)	0.075(5)	0.28(2)	0.001(1)	0.50(2)	0.001(1)
Yb	n.a.	n.a.	11.0(3)	0.38(2)	1.91(8)	0.008(3)	3.8(1)	0.013(4)
Lu	2.0(2)	0.049(9)	2.2(1)	0.043(6)	0.31(3)	n.a.	0.65(3)	0.002(1)

n.a., not analyzed
Values in ( ) represent 1σ uncertainties in the least units cited

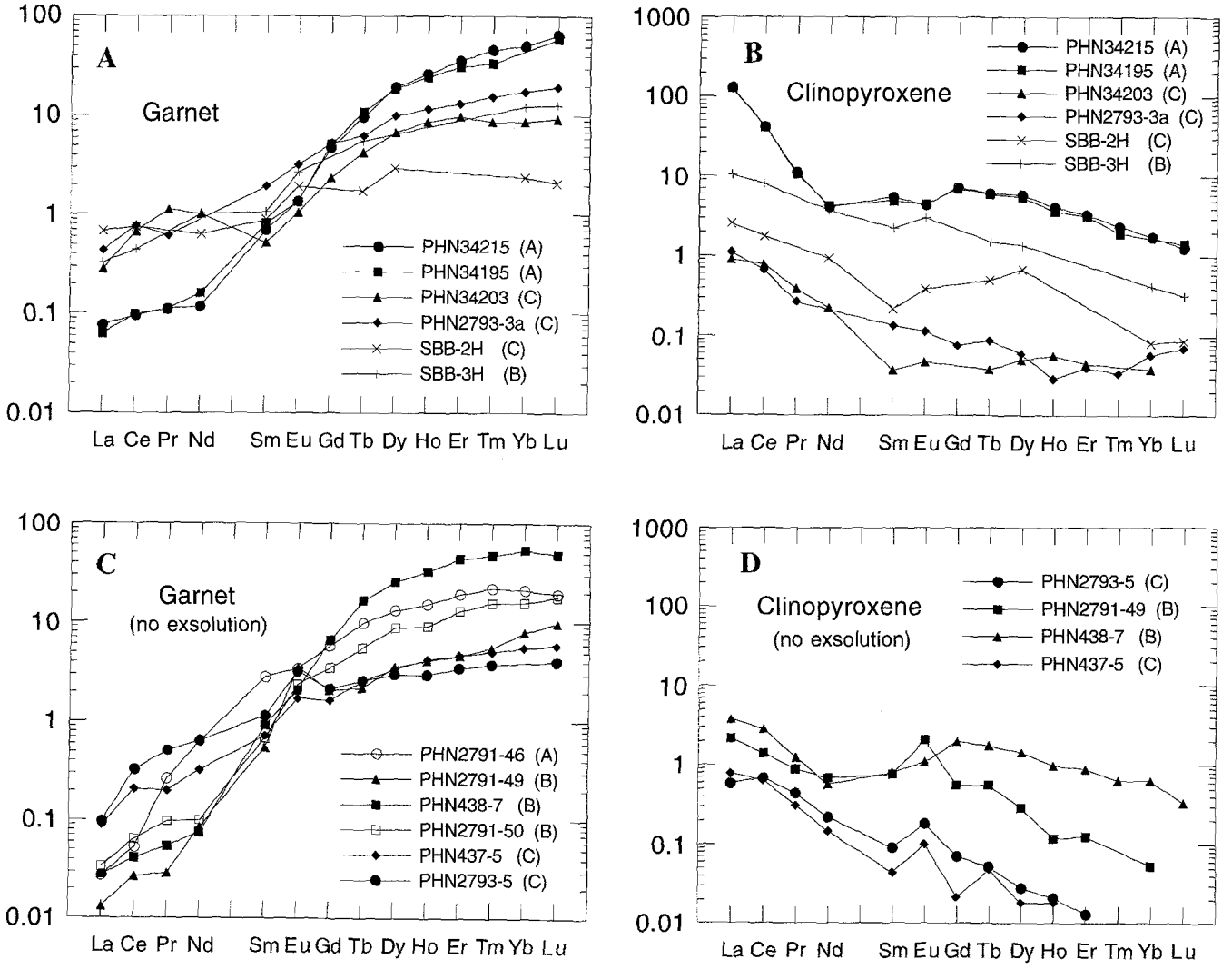

Fig. 3. Chondrite-normalised rare-earth element patterns determined in this study by SIMS for: **A** garnet; **B** clinopyroxene, and for two eclogites with exsolution analyzed by INAA (SBB-2H and 3H; Caporuscio and Smyth 1990). *Letters in* ( ) indicate eclogite groups. Rare-earth element patterns in: **C** garnet; **D** clinopyroxene determined by SIMS for eclogites with no exsolution textures

these samples, considerably less than that (130–270) ascribed to Group A by Taylor and Neal (1989). Three samples (PHN2793-3a, PHN34203, and SBB-2H) contain clinopyroxenes with REE abundances at levels of the Group C xenoliths described by Taylor and Neal (1989). However, the exsolved samples here have $La_N/Yb_N = 19–30$, which is higher than the values of 2–5 found by Taylor and Neal (1989) for eclogites of similar REE abundances.

The two eclogites exhibiting the highest REE abundances (PHN34195 and PHN34215) also contain garnet with the highest HREE abundances (Fig. 3A). This is in contrast to the work of Taylor and Neal (1989), who found that samples containing clinopyroxene enriched in REE (their Group A) have garnet of intermediate HREE abundances. Comparison of our Fig. 3A with Fig. 4a of Taylor and Neal (1989) shows that garnet in PHN34195 and PHN34215 contains HREE at the levels of Group B eclogites (Lu ~ 70–80 × chondrites). Garnets in PHN34203 and 2793-3a have LREE abundances similar to the two samples of Caporuscio and Smyth (1990). One of the samples (SBB-2H) has a nearly flat REE pattern for garnet, although a small amount of contamination coupled with analytical uncertainties may be the cause of this unusual pattern.

Mineral/mineral partition coefficients such as $La_{garnet}/La_{clinopyroxene}$ were investigated to see if the variations in REE compositions could be an expression of differing mode, temperature, or mineral major-element composition. However, no correlations with mode, mineral compositions, or calculated temperatures were observed. Such correlations may exist, but not be discernible because of the poor statistics inherent in using the limited data currently available for eclogites containing exsolution.

No evidence for middle REE enrichment in clinopyroxene is seen in the six analyzed samples. Oberti and Caporuscio (1991) report it in SBB-2H, but the data of Caporuscio and Smyth (1990) for the same sample (used here in Fig. 3B) fail to show this feature. The data of Oberti and Caporuscio (1991) for SBB-2H are identical to that of Caporuscio and Smyth (1990), except for Ce, which in the more recent work is a factor of 3 lower (and La, which is not reported). There is no explanation for these differences, and we have chosen to use the complete REE dataset from Caporuscio and Smyth (1990), which is also identical in all respects for all of the other samples reported in Oberti and Caporuscio (1991).

Unique features such as the elevated HREE in some garnets (relative to Taylor and Neal 1989), anomalous pattern slope in clinopyroxene, and a complete lack of Eu anomalies are possible signatures of exsolved eclogites. Considering the paucity data for rare-earth elements in exsolved eclogites (six samples in all), further study is obviously warranted.

Reconstructed whole-rock "precursor pyroxene" compositions

Based upon the primary modal mineralogy and the mineral compositions (Tables 1–3), it is possible to calculate an approximate whole-rock composition. This composition is sometimes referred to as the "initial" or "precursor" pyroxene (e.g., Harte and Gurney 1975; Smyth et al. 1984, 1989); all of the garnet (and if present, kyanite and corundum) is assumed to have come from clinopyroxene. This, of course, would represent a pyroxenite, which is not an uncommon rock type among mantle xenoliths. Reconstructed compositions are given in Tables 5 and 6, and it is apparent that these would represent aluminous pyroxene compositions, with a substantial Tschemak (CaTs) component indicated by Al^{VI}/Na cation ratios greater than 1. The reconstructed whole-rock compositions are also shown on an AFM diagram in Fig. 4, along with the ordinary eclogites of Smyth and Caporuscio (1984). It is important to note that the exsolved eclogites do not differ significantly in the major elements from ordinary eclogites, except perhaps for a slight alkali enrichment in the exsolved eclogites.

Reconstructed REE compositions are given in Table 6 and shown in Fig. 5, along with data for the two exsolved eclogites from Caporuscio and Smyth (1990). The patterns of Fig. 5 are typical of the reconstructions described by Taylor and Neal (1989), whose Group A has the highest LREE, Group C the lowest. Note, however, that eclogites PHN34195 and PHN34215 have steep LREE slopes (inherited from the clinopyroxene), and the HREE are slightly enriched, resulting in $La_N/Yb_N = 5–8$ here (Yb being interpolated for sample PHN34195), compared to values of 10–24 reported by Taylor and Neal (1989) for their

Table 5. Major-element compositions of reconstructed whole-rocks ("precursor pyroxene")

Group	A PHN2791-a	A PHN34195	A PHN34215	B O-160a	B O-160b	B O-160c	C PHN34203	C PHN2793-3a
SiO_2	46.79	52.57	50.70	38.79	38.15	43.27	46.21	46.68
TiO_2	0.09	0.14	0.13	0.03	0.03	0.04	0.10	0.12
Al_2O_3	14.49	5.86	8.91	34.26	35.89	27.28	22.78	24.18
Cr_2O_3	0.11	0.45	0.40	< 0.03	0.03	0.03	0.03	0.03
FeO	7.99	4.16	5.53	1.46	1.37	1.61	4.58	4.02
MnO	0.25	0.12	0.15	< 0.03	< 0.03	< 0.03	0.09	0.07
MgO	15.92	16.12	16.30	7.62	7.26	8.61	6.24	6.28
CaO	13.09	18.58	16.00	14.86	14.19	15.91	15.28	13.24
Na_2O	0.97	1.66	1.34	2.51	2.47	2.76	4.20	4.95
Total	99.70	99.66	99.46	99.53	99.39	99.51	99.51	99.57

Table 6. Rare-earth composition (in ppm) of reconstructed whole-rocks ("precursor pyroxene")

Group	A PHN34195	A PHN34215	C PHN34203	C PHN2793-3a	C SBB-2H[a]	B SBB-3H[a]
La	34.83	29.29	0.19	0.27	0.31	0.76
Ce	30.06	25.11	0.61	0.58	0.66	1.68
Pr	1.10	0.96	0.09	0.05	n.a.	n.a.
Nd	2.30	1.84	0.37	0.11	0.31	0.98
Sm	0.87	0.82	0.05	0.15	0.08	0.26
Eu	0.31	0.27	0.04	0.09	0.06	0.21
Gd	1.85	1.79	0.32	0.52	n.a.	n.a.
Tb	0.35	0.37	0.10	0.12	0.04	0.25
Dy	2.55	3.37	1.10	1.21	0.43	0.20
Ho	0.52	0.82	0.31	0.31	n.a.	n.a.
Er	1.65	2.94	1.03	1.04	n.a.	n.a.
Tm	0.21	0.49	0.13	0.17	n.a.	n.a.
Yb	n.a.	3.56	0.90	1.35	0.19	2.19
Lu	0.34	0.68	n.a.	0.23	0.03	0.35

n.a., not analyzed

[a] Compositions reconstructed from data in Caprouscio and Smyth (1990) and estimated modes of Smyth and Caprpusico (1984)

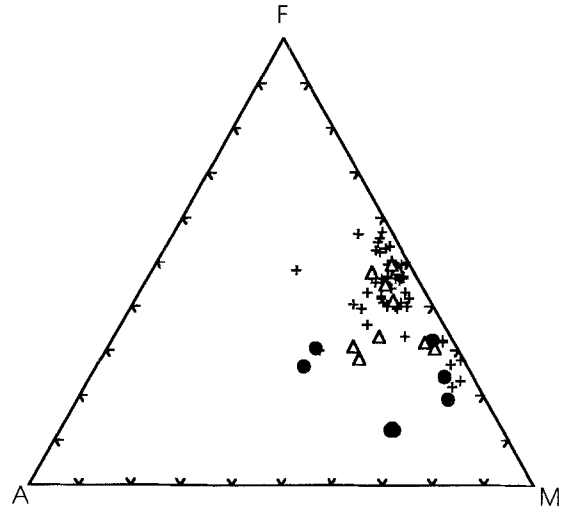

Fig. 4. AFM plot for reconstructed whole-rock compositions showing the similarity of samples with exsolution, *triangles*, *circles*, to those without, *crosses*. Data for this study shown by *filled circles*. Other eclogite data are from Smyth and Caporuscio (1984), with exsolved samples also shown by *triangles*

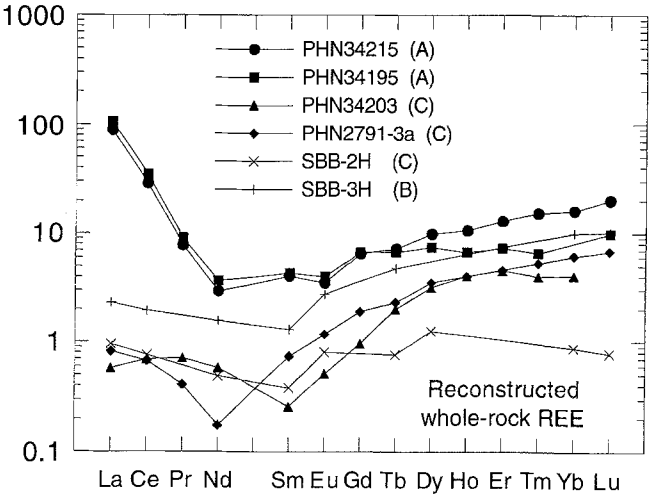

Fig. 5. Chondrite-normalised rare-earth patterns in reconstructed whole-rock compositions. "SBB" samples are reconstructed from chemical data in Caporuscio and Smyth (1990) and the modal data of Smyth and Caporuscio (1984). *Letters in* ( ) indicate eclogite groups

Group A xenoliths which are likewise REE enriched. In the other four samples, which vary in major-element compositions, the basic shapes of the REE patterns are quite similar to each other, unlike those of Taylor and Neal (1989), which show marked differences in the LREE between their Group B and C eclogites. Sample SBB-2H is significantly different, with $La_N/Yb_N = 1.09$, compared with 0.1–0.2 for eclogites of similar composition (Group C) studied by Taylor and Neal (1989). This flat pattern is due to the absence of significant HREE enrichment in the garnets of SBB-2H. In addition, none of the eclogites shown here displays strong Eu anomalies in the reconstructed patterns.

Discussion

The origin of mantle-derived eclogite xenoliths remains the subject of some controversy (e.g., Smyth et al. 1989; Neal and Taylor 1990). Two major hypotheses have been advanced to account for the differences between the eclogite groups. The first is that Group A eclogites formed as magmatic mantle cumulates (e.g., Green 1966; O'Hara and Yoder 1967; Smyth et al. 1989; Taylor and Neal 1989), and Groups B and C, which likely comprise a continuum, are the products of subducted, seawater-altered oceanic-crustal rocks (MacGregor and Manton 1986; Shervais et al. 1988; Taylor and Neal 1989; Neal et al. 1990). In this scheme, Groups B and C may represent the basaltic and feldspathic cumulate portions of the oceanic crust, respectively. A second hypothesis, based on mineral and whole-rock chemistry, is that all three groups formed

through continuous fractionation of a single, evolving magma and that eclogites represent the clinopyroxene cumulate portion of the melt system (Smyth et al. 1989; Caporuscio and Smyth 1990). Isotopic data conflict with this conclusion, however (Shervais et al. 1988; Neal and Taylor 1990; Neal et al. 1990; Pearson et al. 1992). Among exsolved eclogite samples, all three eclogite groups are represented.

Eclogites exhibiting exsolution of garnet are assumed to have had a pyroxenite precursor when calculations of precursor, pyroxenes are made. The aluminous nature of the reconstructed pyroxenes is obvious (Table 5). However, mantle pyroxenes with more than 23–24% Al_2O_3 may be unrealistic. If they are commonly formed, such pyroxenes may only be preserved if erupted soon after formation. Indeed, pyroxenes in eclogites with $> 20\%$ Al_2O_3 are rare. Lappin (1978) reported a Roberts Victor grospydite with pyroxene containing $\sim 20.5\%$ Al_2O_3, and two grospydites from the Zagadochnaya pipe in Siberia have pyroxene with $\sim 22.5\%$ Al_2O_3 (Sobolev 1977). The reconstructed compositions with the highest Al_2O_3 are for samples which also contain abundant kyanite and/or corundum. It is a common practice to include these minerals in the reconstructed precursor pyroxene calculations under the assumption that they formed entirely from pyroxene. It is our view that consideration must be given to the possibility that some of these aluminum-bearing phases were "primary", forming directly from the protolith. Kyanite is described as primary in the Roberts Victor grospydite of Lappin (1978) mentioned above. If the pressures experienced by the protolith during eclogite formation were not much above 30 kbar, a Ca-Eskola component in the pyroxene would not be stable. This component is required before the kyanite (with its lower cation/oxygen ratio) could be an exsolving phase.

Griffin et al. (1979) describe the presence of kyanite needles in plagioclase of granulites, perhaps recording part of the process of conversion to eclogite. If some eclogites do form from granulites, there is a real possibility that plagioclase is consumed in the formation of both kyanite and aluminous clinopyroxene. This kyanite may be partially or totally replaced by garnet through later recrystallization. Cases where kyanite is consumed by garnet are known (e.g., Sobolev et al. 1968; Dawson 1980), and also are preserved in O-160 where kyanite lamellae are partially replaced by garnet.

It is possible that kyanite (and corundum) eclogites may represent protoliths that contained abundant plagioclase. Upon a pressure increase and transformation at depth, the protoliths had excess aluminum, forming kyanite ($\pm$ corundum) in addition to aluminous pyroxene. During exsolution, the CaTs portion of the pyroxene went to form garnet, and garnet may also have consumed some of the primary kyanite. Of course, if a Ca-Eskola component is present in the pyroxene, exsolution may produce kyanite as well. The fact that kyanite (and/or corundum) is only seen in appreciable amounts in the most aluminous samples suggests the existence of a threshold amount of Al_2O_3 in the protolith, above which the final product contains primary kyanite and/or corundum.

The high Al_2O_3 content and positive Eu anomaly usually seen in Group C ordinary eclogites are consistent with an origin as plagioclase-rich crustal cumulates (Taylor and Neal 1989; Taylor et al. 1991). The high Al_2O_3 (22.8% and 24.2%) in the reconstructed whole-rock compositions of PHN34203 and PHN2793-3a (respectively), yet no Eu anomalies (Fig. 3A, B and Fig. 5) suggests that if these do represent plagioclase cumulates, the original plagioclase never had (or lost) the anomaly prior to reequilibriation at mantle depths. This could result from a higher oxygen fugacity at the point of origin of the protolith, which would keep Eu in the 3^+ state and incompatible with plagioclase. Such a fugacity could be the result of interaction with an active hydrothermal system at the time of formation. An alternative explanation for the aluminous nature of the reconstructions may be a protolith containing abundant spinel in addition to clinopyroxene. Such an assemblage is common in Al-augite xenoliths and alpine peridotites. Upon an increase in pressure, this assemblage would form an aluminous pyroxene which, under a continued pressure increase, may later exsolve garnet as the CaTs solubility decreases. The fact that some Group C eclogites are missing the Eu anomaly indicates that such alternative scenarios are important at least locally.

It has been asserted by Smyth et al. (1989) and Caporuscio and Smyth (1990) that grospydites cannot represent metamorphosed feldspathic crust because corundum grospydite compositions contain too much Na and Al_2O_3 ($> 28\%$), and too little K to "...correspond to any known crustal rock type..." (Smyth et al. 1989). However, Archean anorthosites with up to 31% Al_2O_3 are known (Ashwal et al. 1983), and seawater alteration is likely to enrich Na and deplete K. Moreover, Weiblen and Morey (1980) report an anorthosite composition that is corundum normative. The Archean anorthosite compositions given in Ashwal et al. (1983) are also corundum normative if the "losses on ignition" ($\sim 2\%$) are partitioned between Fe and Mg (akin to an anorthosite with a few percent olivine).

The mineral rare-earth patterns (Fig. 3A, B) are somewhat different from those in some of their non-exsolution-containing, ordinary-eclogite counterpart (compare with Shervais et al. 1988; Taylor and Neal 1989; Caporuscio and Smyth 1990). The chondrite-normalized REE patterns for some exsolved eclogite minerals display slopes that are atypical for the ordinary eclogite minerals of similar major-element composition. Another notable difference between exsolved versus ordinary eclogites is the lack of pronounced positive Eu anomalies in the three eclogites with sodic clinopyroxene and calcic garnet (PHN34203, PHN2793-3a, and SBB-2H). These correspond to the Group C eclogites of Taylor and Neal (1989). Positive anomalies are a common feature observed in this group by Shervais et al. (1988) and Taylor and Neal (1989). Positive Eu anomalies were found in both Group B and C eclogites by Taylor et al. (1991; shown in Fig. 3C, D), and work in progress on a large suite of eclogites from Yakutia, Siberia shows positive Eu anomalies in both Group B and C eclogites. Partial melting and fractionation processes in the dynamic upper mantle may add or remove anomalies, confusing the issue and making Eu a poor indicator. Continued study may show that Eu anomalies are not a general characteristic of Group C eclogites,

although Group C may still exhibit the most positive anomalies.

As described previously, the SIMS analyses are from unaltered mineral cores; therefore, the differences from ordinary eclogites cannot be ascribed to metasomatism. It is possible that the mineral differences in this group are due to effects of subsolidus partitioning of elements between the phases. As discussed previously, no systematic variations were observed among garnet/clinopyroxene partition coefficients. This suggests that as exsolution of garnet occurs, a metastable type of partitioning may take place for the REE due to their charge and large ionic radius. The resulting garnet may accept elements in different amounts compared to a system where both garnet and clinopyroxene were forming through recrystallization. As a result, some of the mineral REE patterns, while resembling those of ordinary eclogites, exhibit slight variations in the chondrite-normalized slopes. Compared to ordinary eclogites, the REE patterns for garnet in exsolved eclogites have steeper positive slopes (a slight enrichment in HREE) and less negative slopes for clinopyroxene (greater $[La/Yb]_N$ ratios).

Synopsis

The exsolved samples studied here belong to all three eclogite groups, and no major chemical differences are recognized between samples with exsolution and those without, suggesting that differences between the two suites are principally textural. Rare-earth element patterns are subtly different from ordinary eclogites of corresponding groups, however. The chondrite-normalized REE patterns of clinopyroxenes in exsolved eclogites have flatter HREE patterns, and garnets have elevated HREE relative to ordinary eclogites. These may be exsolution signatures, possibly the result of a metastable partitioning of REE during exsolution.

For the South African eclogites, a model of crustal underplating has been proposed by Basu et al. (1986) and Neal et al. (1990), in which a subducted slab was emplaced beneath the Kaapvaal craton and has remained there for > 2 Gyr. The problems in applying the eclogite classification scheme from Africa to the Siberian samples suggests differences in the mantle between the two regions. There may be no underplated slab below Siberia, and the upper mantle may play a larger role in the direct formation of the eclogites sampled as xenoliths.

The presence of exsolution features is common among mantle lithologies. Aluminous pyroxenes, therefore, must be a typical component of mantle rock precursors. In reconstructing precursor compositions for exsolved eclogites, it is generally assumed that the precursor was a pyroxene. In fact, if this was the case, the extremely Al rich compositions ($> 24\%$ Al_2O_3) for kyanite- or corundum-bearing samples are unusual pyroxenes, rarely seen in mantle rocks. It is more plausible that some of the kyanite and/or corundum formed directly from the protolith (i.e., are primary). It is suggested that for protoliths with more than $\sim 24\%$ Al_2O_3 (e.g., plagioclase cumulates), primary kyanite and corundum are formed directly during conversion to eclogite. In cases where a Ca-Eskola component is present in pyroxene, kyanite lamellae may form in addition to any garnet lamellae.

If the immediate precursor for eclogites typically includes aluminous pyroxene, as is likely, then exsolution of garnet can be expected to have been ubiquitous. However, exsolution textures have been shown to be transient (e.g., Tuttle and Bowen 1958). If many eclogites underwent the exsolution process at some point, the only difference between the two sets of eclogites (exsolved and ordinary) may be that many have lost (via recrystallization?) the evidence of their exsolution.

Appendix

PHN2791-a

Garnet is the predominant mineral, and the exsolution of this phase is either as lamellae or elongate to subequant inclusions. These lamellae and inclusions exhibit a single orientation within a given clinopyroxene crystal. Lamellae range from 50 to 200 μm in width, and inclusions, where elongate, are parallel to lamellae. Locally, the inclusions form aggregates, some of which are parallel to garnet lamellae. Individual blebs are generally from 0.2 to 1.4 mm long and 0.05 to 0.5 mm wide, with aggregates up to 2 mm in length. Non-lamellar garnet includes equant, xeno- to subidiomorphic crystals in the matrix between clinopyroxene grains. These garnet crystals are up to 4.7 mm, although aggregates > 1 cm and enclosing clinopyroxene are also present. Clinopyroxene occurs both as matrix crystals up to 1 cm and as occasional 0.6 to 2 mm inclusions in garnet. Some of these latter pyroxenes are surrounded by the primary garnet crystal aggregates. The principal alteration product of both clinopyroxene and garnet is pale to olive-green phlogopite.

PHN2793-3a

Large areas of phlogopite are present as alteration products of pyroxene, resulting in a blebby appearance for much of the remaining pyroxene. Regions of this pyroxene > 5 mm go to extinction simultaneously, indicating the original grain size. Undulatory extinction is prominent in scattered patches of pyroxene. The pyroxene grains contain inclusions (~ 50 μm) of granular garnet and elongate, but irregular corundum. Garnet is granular or blebby for the most part, with grains from 0.5 to > 3 mm. Garnet exsolution is restricted to one area of the section, and lamellae are commonly over 100 μm wide, although those over > 150 μm appear more lensoid than lamellar. Some of the blebby grains may be exsolved garnet that has been partially recrystallized. Corundum and kyanite are minor phases. Discrete corundum grains are round and elongate, with dimensions commonly of 200×900 μm. Blades of kyanite range from 20×600 μm to 50×200 μm.

PHN34195

This sample is dominated by large crystals of clinopyroxene (up to 1.5 cm). Garnet lamellae are oriented in a single direction within each clinopyroxene crystal, are parallel to orthopyroxene exsolution lamellae, and range up to 40 microns wide. Elongate, discontinuous blebs of garnet are also parallel to orthopyroxene and garnet lamellae and are likely of similar origin. Although most blebs of garnet are elongate (up to 0.4 mm wide and 2.8 mm long), there is a population of smaller garnets (200 to 400 μm) which are essentially equant in the thin section. While these may represent cross sections of spindle-shaped lamellae, they appear more euhedral than the lamellae. It is unclear whether these small garnet inclusions are also exsolved from clinopyroxene or primary. Primary garnet inclusions within matrix clinopyroxene range from 1.6 to 2.6 mm. Crescent-

and lens-shaped crystals of primary garnet up to 4.4 mm are seen between clinopyroxenes. In this section, as in all sections, phlogopite is the dominant alteration product, although a significant amount of serpentine is also present.

PHN34215

This sample is heavily altered and the overall texture is xenomorphic inequigranular. Both blebs and minor lamellae of exsolved garnet are present and most are elongate and parallel. Primary garnet is external to clinopyroxene and consists of both larger (1.5–7 mm) equant, subhedral crystals, and irregular crescent- and lens-shaped (1–2 mm) grains. Clinopyroxene crystals are up to 1 cm and exhibit irregular outlines. Orthopyroxene lamellae are common and many are extensively altered. In addition to abundant serpentine along grain boundaries and fractures, phlogopite, calcite, chlorite, pale-green amphibole, and fine-grained clay minerals are present as alteration products.

PHN34203

Clinopyroxene is coarse (2–15 mm), irregularly shaped, and exhibits no preferred orientation. This sample is notable for the significant amount ($\sim$3.2%) of corundum present, distributed throughout the section. Orthopyroxene lamellae are present within the clinopyroxene. Garnet lamellae are parallel, and range in width from 20 to 300 μm, with a bimodality in widths. There are two groups of garnet lamellae, each with its own orientation, separated by an apparent angle of $\sim$18°. These two groups coincide with the two width populations, the narrower lamellae (< 150 μm) being parallel to the orthopyroxene and corundum lamellae. This orientation is parallel to {100} of clinopyroxene. The thicker set of lamellae (> 150 μm) may be parallel to {010}, an orientation observed by Smyth et al. (1984). The 18° angle seen in thin section thus would result from the plane of the thin section cutting these obliquely. Primary garnet occurs as anhedral inclusions (up to 2.2 mm) in clinopyroxene as well as larger (2–5 mm) anhedral to subhedral grains often in crystal aggregates. Some euhedral garnet grains up to 1.2 mm are present. Most corundum is seen as inclusions in garnet or clinopyroxene. Corundum is elongate, forming crude "lamellae" that are not as uniform as their garnet counterparts. Patches of corundum are also present, as are elongate grains ("football"-shaped) that occur in chains parallel to lamellae. Where both garnet and corundum are present in the same clinopyroxene, the exsolution appears chaotic, with no consistent texture.

O-160

This sample has been termed a corundum eclogite by Sobolev (1977), because of abundant grains of pink corundum (ruby) up to 2 mm across. Sample O-160 is a xenolith with dimensions of approximately 7×15 cm, and exhibits modal layering (photo 4a of Sobolev 1977) and prominent exsolution lamellae. A roughly circular slab $\sim$7 cm across was obtained from the xenolith (from the left side in photo 4a of Sobolev 1977). The three samples analyzed here were taken from different portions across the slab to determine what variations (if any) exist.

All three portions are similar, having coarse clinopyroxene grains up to 1.5 cm, some extensively fractured. Garnet lamellae are generally 50–75 μm, but are present up to 125 μm across. In O-160c garnet lamellae 200 μm wide are seen. While usually linear, individual lamellae display widely varying widths along their length. Garnet grains are present, but rare, and 500–1,000 μm across. Kyanite lamellae are common in portions of the sample and are thin, typically being 5–10 μm wide, the largest being approximately 20 μm. Kyanite lamellae are not as uniformly straight as the garnet ones, exhibiting abundant short appendages (resembling "flame" structures seen in some sediments) and occasional offsets. In general, the kyanite is consistent in orientation with garnet, although one area of sample O-160a has chaotically oriented kyanite lamellae. Locally, kyanite lamellae are interrupted by garnet, the interceding garnet lamellae being wider. In O-160b, there are remnants of the kyanite lamellae within the garnet. These remnants are discontinuous and often bead like, with "beads" usually < 5 μm. It seems likely that the garnet formed in these areas by consuming kyanite. The number of kyanite lamellae is greatest in O-160b. Corundum is present as both equant and rod-shaped grains. Equant grains are present up to $\sim$2 mm across, and rods to 3 mm are present. Corundum comprises up to 20% of the rock and is disseminated fairly evenly within each sample. Orthopyroxene was not observed petrographically. Alteration products are minor in abundance, being most common in O-160c. Phlogopite is the principal alteration mineral, affecting pyroxene in general, and seen in garnet only in the garnet grains (i.e., not affecting the lamellae).

Acknowledgments. We are grateful to P.H. Nixon for furnishing the eclogite samples from the Bellsbank kimberlite. Allan Patchen, Pung Huang, and Jim Eckert assisted in the electron microprobe analyses and data manipulation. Yuequn Jin and Qu Qi aided in thin section preparation. Thanks also go to Clive Neal and Emil Jagoutz for helpful discussions, and to Doug Smith and two anonymous reviewers of the original manuscript for helpful suggestions. The ion microprobe analyses were supported by NSF grant EAR 9017587 to G. Crozaz. In addition, a portion of this study was supported by NSF grant EAR 9118043 to L.A. Taylor.

References

Aoki K-I, Fujimaki H, Kitamura M (1980) Exsolved garnet-bearing megacrysts from some South African kimberlites. Lithos 13:269–279

Ashwal LD, Morrison DA, Phinney WC, Wood J (1983) Origin of Archean anorthosites: evidence from the Bad Vermillion Lake anorthosite complex, Ontario. Contrib Mineral Petrol 82:259–273

Basu AR, Ongley JS, MacGregor ID (1986) Eclogites, pyroxene geotherm, and layered mantle convection. Science 233:1303–1305

Bobrievich AP, Smirnov GI, Sobolev VS (1960) The mineralogy of xenoliths of a grossular-pyroxene-disthene rock (grospydite) from the Yakutian kimberlites (in Russian). Geol Geofiz 3:18–24

Borley GD, Suddaby P (1975) Stressed pyroxenite nodules from the Jagersfontein kimberlite. Mineral Mag 40:6–12

Caporuscio FA, Smyth JR (1990) Trace element crystal chemistry of mantle eclogites. Contrib Mineral Petrol 105:550–561

Carswell DA, Dawson JB, Gibb FGF (1981) Equilibration conditions of upper-mantle eclogites: implications for kyanite-bearing and diamondiferous varieties. Mineral Mag 44:79–89

Coleman RG, Lee DE, Beatty LB, Brannock WW (1965) Eclogites and eclogites: their differences and similarities. Geol Soc Am Bull 76:483–508

Dawson JB (1980) Kimberlites and their xenoliths. Springer, Berlin Heidelberg New York

Desnoyers C (1975) Exsolutions d'amphibole, de grenat et de spinelle dans les pyroxenes de roches ultrabasiques: peridotites et pyroxenolites. Bull Soc Fr Mineral Cristalogr 98:65–72

Freer R, Carpenter MA, Long JVP, Reed SJB (1982) "Null result" diffusion experiments with diopside: implications for pyroxene equilibria. Earth Planet Sci Lett 58:285–292

Gasparik T (1984) Experimentally determined stability of clinopyroxeneegarnet + corundum in the system CaO-MgO-Al_2O_3-SiO_2. Am Mineral 69:1025–1035

Green DH (1966) The origin of "eclogites" from Salt Lake Crater Hawaii. Earth Planet Sci Lett 9:367–389

Griffin WL, Carswell DA, Nixon PH (1979) Lower-crustal granulites and eclogites from Lesotho, southern Africa. In: Boyd FR, Meyer HOA (eds) The mantle sample: inclusions in kimberlites and other volcanics, vol 2. Am Geophys Union, Washington, DC, pp 59–86

Harte B, Gurney JJ (1975) Evolution of clinopyroxene and garnet in an eclogite nodule from the Roberts Victor kimberlite pipe, South Africa. Phys Chem Earth 9:367–387

Hays JF (1966) Lime-alumina-silica. Carnegie Inst Washington Yearb 65:234–239

Jagoutz E (1988) Nd and Sr systematics in an eclogite xenolith from Tanzania: evidence for frozen mineral equilibria in the continental lithosphere. Geochim Cosmochim Acta 52:1285–1293

Jagoutz E, Carlson RW, Lugmair GW (1980) Equilibrated Nd-unequilibrated Sr isotopes in mantle xenoliths. Nature 286:708–710

Kurat G, Palme H, Spettel B, Baddenhausen H, Hoffmeister H, Palme C, Wanke H (1980) Geochemistry of ultramafic xenoliths from Kapfenstein, Austria; evidence for a variety of upper mantle processes. Geochim Cosmochim Acta 44:45–60

Lippin MA (1978) The evolution of a grospydite from the Roberts-Victor mine, South Africa. Contrib Mineral Petrol 66:229–241

Lappin MA, Dawson BD (1975) Two Roberts-Victor cumulate eclogites and their re-equilibration. Phys Chem Earth 9:351–365

Lundberg LL, Crozaz G, McKay G, Zinner E (1988) Rare earth element carriers in the Shergotty meteorite and implications for its chronology. Geochim Cosmochim Acta 52:2147–2163

Lundberg LL, Crozaz G, McSween HY (1990) Rare earth elements in minerals of the ALHA 77005 shergottite and implications for its parent magma and crystallization history. Geochim Cosmochim Acta 54:2535–2547

MacGregor ID, Manton WI (1986) The Roberts-Victor eclogites: ancient oceanic crust. J Geophys Res 91:14063–14079

McCormick TC (1984) Crystal chemistry and breakdown reactions of aluminous mantle-derived omphacites. PhD dissertation, Arizona State Univ

Neal CR, Taylor LA (1990) Comment on "Mantle eclogites: evidence of igneous fractionation in the mantle" by JR Smyth, FA Caporuscio, and TC McCormick. Earth Planet Sci Lett 101:112–119

Neal CR, Taylor LA, Davidson JP, Holden P, Halliday AN, Nixon PH, Paces JB, Clayton RN, Mayeda TK (1990) Eclogites with oceanic crustal and mantle signatures from the Bellsbank kimberlite, South Africa, part 2: Sr, Nd, and O isotope geochemistry. Earth Planet Sci Lett 99:362–379

Oberti R, Caporuscio FA (1991) Crystal chemistry of clinopyroxenes from mantle eclogites: a study of the key role of the M2 site population by means of crystal-structure refinement. Am Mineral 76:1141–1152

O'Hara MJ, Yoder HS (1967) Formation and fractionation of basic magmas at high pressure. Scott J Geol 3:67–117

Pearson DG, Shirey SB, Carlson RW, Taylor LA (1992) Os isotope constraints of the petrogenesis of eclogite xenoliths. AGU 1992 Spring Meeting, Trans Am Geophys Union EOS 73: 376

Sautter V, Harte B (1988) Diffusion gradients in an eclogite xenolith from the Roberts-Victor kimberlite pipe; I: mechanism and evolution of garnet exsolution in Al_2O_3-rich clinopyroxene. J Petrol 29:1325–1352

Sautter V, Harte (1990) Diffusion gradients in an eclogite xenolith from the Roberts-Victor kimberlite pipe: (2) kinetics and implications for petrogenesis. Contrib Mineral Petrol 105:637–649

Shervais JW, Taylor LA, Lugmair GW, Clayton RN, Mayeda TK, Korotev RL (1988) Early Proterozoic oceanic crust and the evolution of subconinental mantle: ecologites and related rocks from southern Africa. Geol Soc Am Bull 100:411–423

Smyth JR, Caporuscio FA (1984) Petrology of a suite of eclogite inclusions from the Bobbejaan kimberlite, II: primary phase compositions and origin. In: Kornprobst J (ed) Kimberlites II: the mantle and crust-mantle relationships. Elsevier, Amsterdam, pp 121–131

Smyth JR, McCormick TC, Caporuscio FA (1984) Petrology of a suite of eclogite inclusions from the Bobbejaan kimberlite, I: two unusual corundum-bearing kyanite eclogites. In: Kornprobst J (ed) Kimberlites II: the mantle and crust-mantle relationships. Elsevier, Amsterdam, pp 121–132

Smyth JR, Caporuscio FA, McCormick TC (1989) Mantle eclogites: evidence of igneous fractionation in the mantle. Earth Planet Sci Lett 93:133–141

Sobolev NV (1977) Deep-seated inclusions in kimberlites and the problem of the composition of the upper mantle. Am Geophys Union, Washington, D.C.

Sobolev VS, Sobolev NV (1964) Xenoliths in kimberlites of northern Yakutia and the structure of the mantle. Dok Akad Nauk SSSR Ser Seol 158:22–26

Sobolev NV, Kuznetsova IK, Zyuzin NI (1968) The petrology of grospydite xenoliths from the Zagadochnaya kimberlite pipe in Yakutia. J Petrol 9:253–280

Stosch H-G (1982) Rare earth element partitioning between minerals from anhydrous spinel peridotite suites from Dreiser Weiher, West Germany. Geochim Cosmochim Acta 46:793–812

Taylor LA, Neal CR (1989) Eclogites with oceanic crustal and mantle signatures from the Bellsbank kimberlite South Africa, part I: mineralogy, petrography, and whole rock chemistry. J Geol 97:551–567

Taylor LA, Eckert JO, Neal CR, Crozaz G (1991) Crustal signatures in mantle eclogites: REE patterns of clinopyroxene and garnet by SIMS and INAA (abstract). 5th Int Kimb Conf extended abstr, CPRM Spec Publ 2/91, Brasilia, pp 410–414

Tuttle OF, Bowen NL (1958) Origin of granite in the light of experimental studies in the system $NaAlSi_3O_8$-$KAlSi_3O_8$-SiO_2-H_2O. Geol Soc Am Mem 74

Weiblen PW, Morey GB (1980) A summary of the stratigraphy, petrology, and structure of the Duluth Complex. Am J Sci 280-A: 88–133

Zinner E, Crozaz G (1986) A method for the quantitative measurement of rare earth elements in the ion microprobe. In J Mass Spectrom Ion Processes 69:17–38

Editorial responsibility: T. Grove